International Journal of Pharmacology

Int. J. Pharmacol. **2026**; 22(4): 48608
https://doi.org/10.31083/IJP48608

Research Article

Mechanism Investigation of *Sophora davidii* Flower Extract Against LPS-Induced Acute Lung Injury Based on Network Pharmacology and Molecular Dynamics Simulation

Cheng Lin[1], Xue Wang[1], Daoyuan Li[1], Ping Chen[1], Baibai Ye[1], Linfu Li[1,*]

[1]Jiangxi Province Key Laboratory of Pharmacology of Traditional Chinese Medicine, Gannan Medical University, 341000 Ganzhou, Jiangxi, China
*Correspondence: lflfllf2001@126.com (Linfu Li)

Academic Editor: Mehmet Ozaslan
Submitted: 27 November 2025 Revised: 4 March 2026 Accepted: 17 March 2026 Published: 4 August 2026

Abstract

Aim: Acute lung injury (ALI) is a common respiratory disease that significantly contributes to morbidity and mortality. *Sophora dav*idii flower extract (SDFE), used both as a vegetable and a traditional medicine, has shown potential to alleviate ALI, but the associated underlying mechanisms remain unknown. This study aimed to elucidate the mechanisms through which SDFE protects against ALI. **Methods**: Key signaling pathways, molecular targets, and bioactive compounds associated with the anti-ALI effects of SDFE were predicted using network pharmacology. Lipopolysaccharide (LPS)-induced ALI models were established in BEAS-2B cells and rats. The protective effects of SDFE were investigated by measuring the tissue injury markers alkaline phosphatase (ALP) and lactate dehydrogenase (LDH) in lung tissue and bronchoalveolar lavage fluid (BALF). Representative proteins in the main pathways were validated using molecular docking, molecular dynamics simulation, and experimental assays. **Results**: Network pharmacology analysis identified 363 SDFE targets closely associated with ALI, including the endothelial injury markers intercellular adhesion molecule-1 (ICAM-1) and vascular cell adhesion molecule-1 (VCAM-1). The results of molecular docking and molecular dynamics simulations demonstrated that ICAM-1 and VCAM-1 have strong binding affinity for quercetin and matrine. Kyoto Encyclopedia of Genes and Genomes (KEGG) pathway analysis indicated that leukocyte adhesion and oxidative stress are two key signaling pathways involved in the therapeutic effects of SDFE against ALI. SDFE significantly reduced ALP, LDH, and nitric oxide (NO) levels in lung tissue and BALF from ALI rats and markedly inhibited neutrophil elastase (NE) and myeloperoxidase (MPO) expression in lung tissue. In LPS-stimulated BEAS-2B cells, SDFE downregulated the mRNA expression of *ICAM-1* and *VCAM-1*, the protein expression of MPO, and the level of NO. **Conclusions**: SDFE can ameliorate LPS-induced ALI by inhibiting leukocyte adhesion and reducing oxidative stress.

Keywords: acute lung injury; *Sophora davidii* (Franch.) skeels; flower extract; network pharmacology; leukocyte adhesion; oxidative stress

1. Introduction

As is well known, acute lung injury (ALI) is an acute inflammatory lung disease caused by multiple factors, leading to cell damage of pulmonary microvascular endothelium and alveolar epithelium, resulting in diffuse interstitial pulmonary edema [1]. Severe ALI may progress to acute respiratory distress syndrome (ARDS), a condition marked by refractory hypoxemia, acute respiratory distress, and bilateral pulmonary infiltrates [2]. The incidence and mortality rates of ALI/ARDS are high. A study investigating 23,280 patients in 145 pediatric intensive care units across 27 countries found that the incidence and mortality rates of ALI in 2016–2017 were 17% and 3.2%, respectively [3].

ALI poses a serious threat to human health. The pathogenesis of ALI has multiple possible mechanisms, which vary according to the underlying cause. It is widely accepted that uncontrolled local or systemic inflammation is a major pathophysiological mechanism of ALI [4]. Inflammation can increase the protein expression of some cell adhesion molecules, such as ICAM-1 and VCAM-1 [5,6]. It has been reported that ICAM-1 and VCAM-1 are primarily expressed on the surface of endothelial cells and alveolar epithelial cells, and through binding with their ligands, they mediate the adhesion of inflammatory cells to lung tissue cells, further exacerbating inflammation and inducing oxidative stress [7]. Oxidative stress also plays a critical role in the development and progression of ALI [8,9]. The overproduction of reactive oxygen species (ROS) beyond the capacity for clearance increases membrane permeability, damages the alveolar and vascular endothelium, disrupts the microvascular barrier, reduces alveolar fluid clearance, and aggravates pulmonary edema [10,11,12]. Inhibition of cell adhesion and oxidative stress can improve ALI.

The prevention and treatment of ALI have long been a major focus in the medical field. ALI can be treated with mechanical ventilation and pharmacological therapy. Pharmacological treatments typically include corticosteroids and anti-infective agents. However, long-term use of these drugs may lead to various side effects. For example, dexamethasone, which is widely used in clinical treatment of ALI, can cause osteoporosis and gastrointestinal ulcers [13]. Traditional Chinese medicine (TCM) has been used

for thousands of years, and its safety profile is relatively high. In recent years, more and more studies have reported that TCM can improve ALI. Various components and extracts of TCM exhibit anti-inflammatory and protective effects in ALI intervention. For example, rutin has shown the ability to alleviate LPS-induced acute lung injury by inhibiting the activation of oxidative stress pathway and the MAPK- NF-κB pathway, which will prevent the expression of VCAM-1 and MDA [14,15]. Searching for safe and effective TCM treatments for ALI has become a preferred strategy.

Sophora davidii is predominantly found in China's Yunnan and Guizhou provinces [16], where its flowers are used both as a vegetable and in traditional medicine. It contains a variety of alkaloids and flavonoids, and is known for heat-clearing, detoxifying, and blood-cooling [17]. The flower extract of *Sophora davidii* (SDFE) is commonly used to treat diseases such as pharyngalgia, inflammation-induced cough, and other respiratory ailments. Previous studies have demonstrated that SDFE alleviates leukocyte infiltration, pulmonary edema, lung injury, and cough in LPS-induced rats [18]. SDFE also has the potential to alleviate ALI, but its mechanism remains unclear. This study aims to use network pharmacology to predict how SDFE exert its anti-ALI effects, and to validate these findings through *in vitro* and *in vivo* experiments.

2. Materials and Methods

2.1 Predicting Potential Mechanisms of SDFE in Treating ALI by Network Pharmacology

The chemical components of SDFE were analyzed using UHPLC-Q-Exactive-Orbitrap-MS/MS (Thermo Scientific, Sunnyvale, California, USA). After filtering, 54 compounds that met the ADME criteria were selected. Their potential targets were predicted using the SwissTargetPrediction database (https://www.swisstargetprediction.ch/). A total of 624 SDFE targets were obtained. ALI targets were retrieved by searching the GeneCards database (https://www.genecards.org/) with the keyword of "acute lung injury". ALI targets (score $\geq$10) from GeneCards were obtained. Using the interactivenn online tool (https://www.interactivenn.net/index2.html), overlapping SDFE and ALI targets (namely intersection targets) were identified and designated as potential therapeutic targets for SDFE against ALI.

Gene Ontology (GO) and Kyoto Encyclopedia of Genes and Genomes (KEGG) enrichment analyses were performed using Metascape V3.5 (https://www.metascape.org) by inputting intersection targets. The top 20 GO terms and KEGG pathways, ranked by p value, were selected for visualization. After targets and compounds related to lipid and atherosclerosis were found out, a protein-protein interaction (PPI) network was generated via the STRING12.0 database (https://cn.string-db.org/) for Homo sapiens under default parameters, and top 30 hub targets were ranked by edge in PPI network. In addition, a compound–target–pathway network was constructed.

The three-dimensional structures of core targets of ICAM-1 (PDB ID: 2OZ4) and VCAM-1 (PDB ID: 1VSC) were retrieved and obtained from the RCSB Protein Data Bank (https://www.rcsb.org/), and the two-dimensional and three-dimensional structures of ligands (quercetin and matrine) were downloaded from the PubChem database (https://pubchem.ncbi.nlm.nih.gov/) simultaneously. Molecular docking of the two ligands with three core targets, followed by visualization, was performed using the LibDock module in Discovery Studio 2019 (Dassault Systèmes, San Diego, California, USA), and the binding affinity of ligands to core target proteins was evaluated using LibDockScore.

A 100 ns molecular dynamics simulation of the protein-ligand complex was conducted by Future Computing Studio using Gromacs 2025 (GROMACS Development Team, Uppsala, Sweden). The system was parameterized with the AMBER14SB (protein) and GAFF2 (ligand) force fields. The complex was solvated with TIP3P water in a cubic box under periodic boundary conditions, and neutralized with 0.15 M Na^+/Cl^- ions. Following energy minimization, the system was equilibrated for approximately 2 ns. The production run lasted 100 ns with a 2 fs time step, under constant temperature (310 K) and pressure (1 bar). Trajectories were saved every 100 ps. Subsequent analyses included binding free energy calculation via molecular mechanics poisson-boltzmann surface area (MMPBSA) and root-mean-square deviation (RMSD) evaluation using GROMACS tools.

2.2 Drugs and Reagents

The dried flowers were obtained from the medicinal materials market of Yunnan Province, and were identified as *Sophora davidii* (Franch.) by Professor Hu Haibo of Gannan Medical University. The voucher specimen has been deposited in the herbarium under the number GMU-S-20230401. The flowers of *Sophora davidii* were processed into SDFE, and its chemical profile (analyzed via UPLC-MS/MS) has been detailed in a previous publication [19]. Aspirin tablets (Bayer HealthCare Co., Ltd., Leverkusen, Germany) and lipopolysaccharide (LPS; Sigma Aldrich, Saint Louis, Missouri, USA) were used in this study.

The main reagents used in the study were as follows: paraformaldehyde solution (Shenzhen Baikai Mei Biotechnology Co., Ltd., Shenzhen, China); nitric oxide assay kit (Shanghai Biyun Tian Biological Technology Co., Ltd., Shanghai, China); ALP and LDH colorimetric assay kits (Wuhan Elabscience Biotechnology Co., Ltd., Wuhan, China); and the RIPA lysis buffer (Beijing Solabio Technology Co., Ltd., Beijing, China).

2.3 LPS-Induced ALI Models in BEAS-2B Cells and Rats

The cell line of BEAS-2B (Shanghai Fuheng Biotech Co., Ltd., Shanghai, China) belongs to human bronchial

epithelial cell line, which was used within passages 3–5. The BEAS-2B line was validated by STR profiling, and the quantitative real-time PCR results showed BEAS-2B line was mycoplasma-free. These cells were cultured in DMEM (low-glucose) supplemented with 10% FBS and incubated at 37 °C with 5% CO_2 in a constant-temperature incubator (Thermo Fisher Scientific, Waltham, MA, USA). BEAS-2B cells were seeded in 60 mm culture dishes (4×10^5 cells per dish) and allowed to adhere for 24 hours. After discarding the medium, the wells were washed with phosphate-buffered saline (Solarbio, Beijing, China) and then incubated for an additional 24 hours. Cells were first incubated with aspirin (5 mM) or SDFE (0.5 or 1 mg/mL) for 6 h, followed by LPS stimulation (5 µg/mL) for an additional 12 h. After centrifugation, supernatants were collected for ELISA and nitric oxide quantification, and cells were harvested for RT-qPCR and western blotting to determine gene and protein expression levels.

30 male Sprague-Dawley rats (4–6 weeks of age, weighing 180–200 g, specific pathogen-free grade) were obtained from Hunan Slaikejingda Experimental Animal Co., Ltd., located in Hunan Province, China. Following a 7-day acclimation period, animals were randomly allocated into five cohorts (n = 6 per group): control, model (LPS, 5 mg/kg), low-dose SDFE (LPS + LD-SDFE, 1.5 g crude drug/kg), high-dose SDFE (LPS + HD-SDFE, 3 g crude drug/kg), and aspirin (LPS + Aspirin, 20 mg/kg). All treatments were orally administered once daily for three consecutive days; control and model groups received an equivalent volume of sterile 0.9% saline. At 2 h post-final administration, ALI was induced in all but the control group by intranasal instillation of LPS (5 mg/kg). Six hours thereafter, rats were euthanized by intraperitoneal injection of 5% sodium pentobarbital (200 mg/kg), and bronchoalveolar lavage fluid (BALF) as well as lung tissues were harvested for subsequent histopathological evaluation, ELISA, and western blot analysis. Throughout the experiment, animals were maintained under specific pathogen-free conditions with temperature (22 ± 2 °C), humidity (55 ± 5%), and a 12 h light/dark cycle rigorously controlled. The study was carried out in accordance with the ARRIVE guidelines. All experimental protocols were reviewed and authorized by the Animal Ethics Committee of Gannan Medical University.

2.4 In Vivo Validation of the ALI-Treating Mechanism of SDFE

2.4.1 Measurement of ALP and LDH in Tissues and BALF

ALP and LDH activities were measured colorimetrically following the protocols supplied with the respective commercial kits. Standard solutions, test samples (from tissues and BALF), and necessary working solutions were prepared. A BCA assay was employed to determine the protein content in tissue homogenates. The standard and sample solutions were separately added to a 96-well plate, followed by the addition of the working solution. The plate was shaken for 10 seconds and incubated at 37 °C for 15 minutes. After adding the color developer, optical density readings were taken at 520 nm using a microplate reader.

2.4.2 Western Blot for MPO

RIPA buffer and BCA protein assay kit (Beijing Solabio Technology Co., Ltd., Beijing, China) were used to lyse lung tissues and quantify and protein extracts, respectively. Equal amounts of protein were resolved by SDS-PAGE on a Bio-Rad electrophoresis system (Mini-PROTEAN Tetra 2-gel Precast System, Bio-Rad Laboratories, Hercules, CA, USA). Wet electrophoretic transfer was employed to immobilize proteins onto PVDF membranes (0.45 µm, Sigma Aldrich, USA) using a Bio-Rad transfer system (USA). The membranes were blocked with skim milk (Shanghai Biyuntian Biotechnology Co., Ltd., Shanghai, China) for 1 hour and incubated overnight at 4 °C with primary antibodies. Primary antibodies for MPO (Cat# DF12528) and β-actin (loading control, Cat# T0022) were sourced from Affinity Bioscience (OH, USA), and used at dilutions of 1:1000 and 1:10,000 respectively. After incubation with secondary antibodies for at least 1 hour, the protein bands were detected using a chemiluminescence gel imaging system (Thermo Fisher Scientific Inc., Waltham, MA, USA). Image J (1.46r, National Institutes of Health, Bethesda, MD, USA) was employed to quantify the optical density of the visualized protein signals.

2.4.3 Immunohistochemistry (IHC) for MPO and NE in Lung Tissues

Following deparaffinization, antigen unmasking was carried out on tissue sections using a microwave oven and an antigen retrieval solution. After cooling, 0.3% Triton X-100 solution (Beijing Solabio Technology Co., Ltd., Beijing, China) was applied, and sections were incubated for 30 minutes. Endogenous peroxidase activity was blocked using a peroxidase blocking agent (Xilong Scientific Co., Ltd., Shantou, China) for 10 minutes. Goat serum (Beijing Solabio Technology Co., Ltd., Beijing, China) was added for 30 minutes at 37 °C. Incubation with primary antibody was carried out at 4 °C overnight; thereafter, sections were treated with secondary antibody at 37 °C for 30 minutes. The reaction was developed with DAB chromogenic solution (Wuhan Elabscience Biotechnology Co., Ltd., Wuhan, China) for 5 minutes. Sections were then counterstained with hematoxylin (Beijing Solabio Technology Co., Ltd., Beijing, China) for 30–60 seconds and washed with purified water. Ammonia water was used to bluing, followed by dehydration and sealing. Stained sections were examined under a light microscope, and quantitative analysis was performed using Image J software.

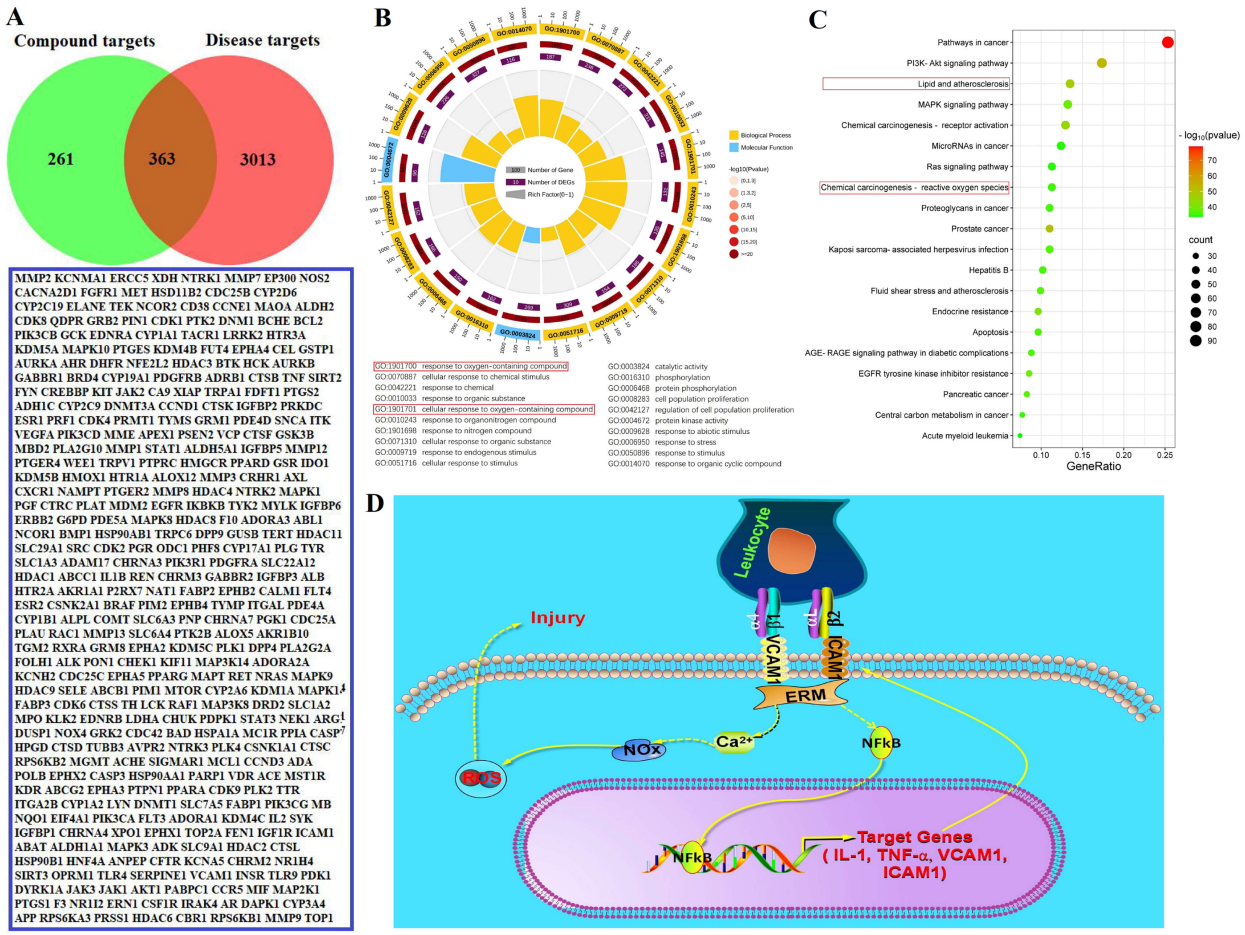

Fig. 1. Predicted mechanisms of SDFE in treating ALI predicted by network pharmacology. (A) ALI-related targets of 54 compounds from SDFE. (B) The 20 most significant GO items from GO enrichment analysis. (C) The 20 most significant KEGG pathways from KEGG enrichment analysis. (D) Subpathway of lipid and atherosclerosis of KEGG pathway: leukocyte transendothelial migration. SDFE, *Sophora davidii* flower extract; ALI, Acute lung injury; GO, Gene Ontology; KEGG, Kyoto Encyclopedia of Genes and Genomes.

2.4.4 Griess Assay for Nitric Oxide (NO)

Nitric oxide content in lung tissues was measured following the instructions provided with the nitric oxide assay kit (Shanghai Biyun Tian Biological Technology Co., Ltd., Shanghai, China).

2.5 In Vitro Validation of the ALI-Treating Mechanism of SDFE

2.5.1 Griess Assay for NO

Cells were processed following the protocol provided with the nitric oxide assay kit (Shanghai Biyun Tian Biological Technology Co., Ltd., Shanghai, China), and the supernatants were collected. After transferring both standards and supernatants to 96-well plates, Griess reagent was applied to each well. The resulting chromophore was quantified by measuring OD540 with a microplate reader.

2.5.2 Western Blot for MPO

RIPA buffer served as the lysis medium for total protein extraction from cells; protein concentrations were subsequently determined with the BCA Protein Assay Kit. The protein samples were then processed according to the standard Western blot procedure previously described.

2.5.3 RT-qPCR for VCAM-1 and ICAM-1

An RNA extraction kit (Beijing ComWin Biotech Co., Ltd., Beijing, China) was utilized to harvest RNA from cell samples, with all steps performed according to the accompanying instructions. The extracted RNA was reverse transcribed into cDNA using a reverse transcription kit (Beijing ComWin Biotech Co., Ltd., Beijing, China). Specific primers for ICAM-1 (forward: 5′-ATGCCCAGACATCTGTGTCC-3′, reverse: 5′-GGGGTCTCTATGCCCAACAA-3′), VCAM-1 (forward: 5′-GGGAAGATGGTCGTGATCCTT-3′, reverse: 5′-TCTGGGGTGGTCTCGATTTTA-3′), and β-

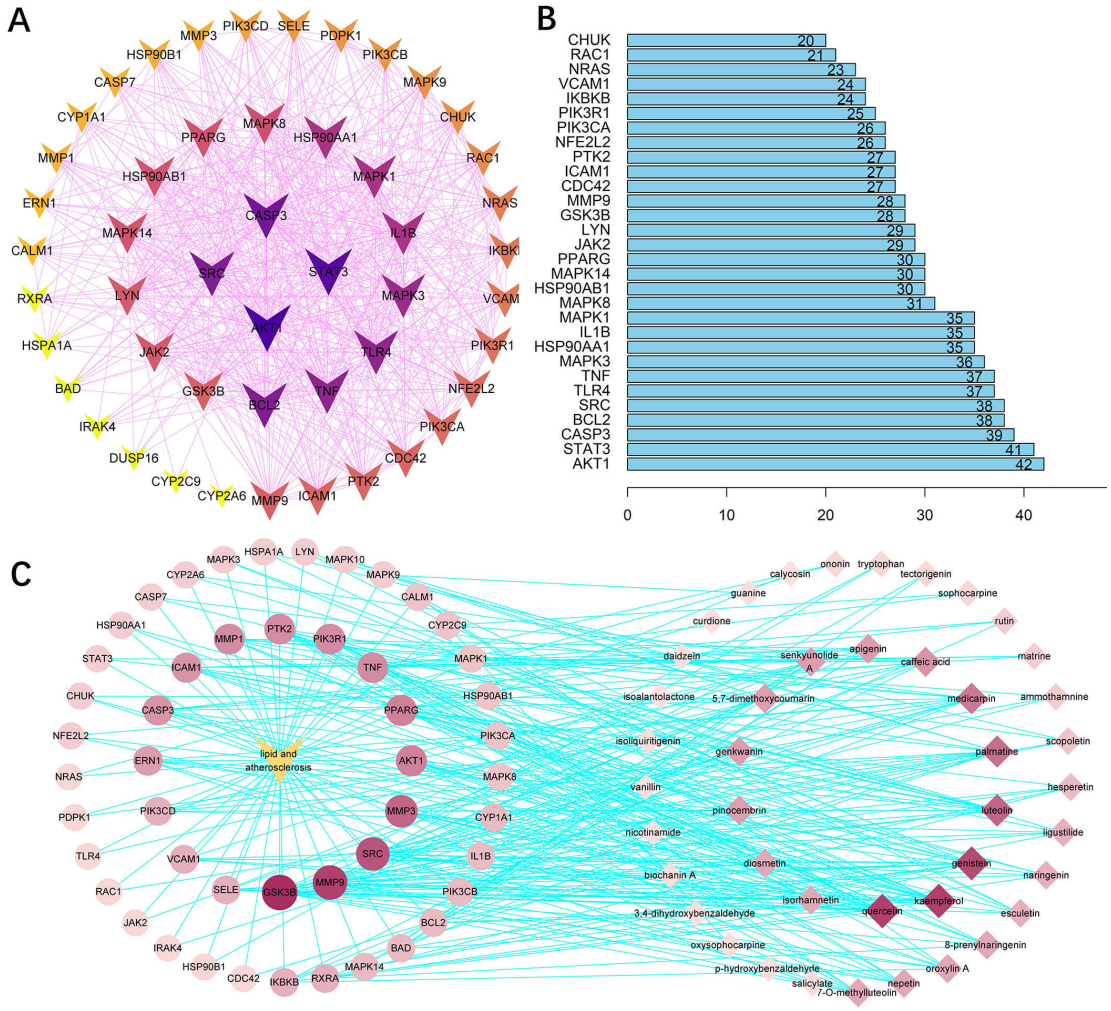

Fig. 2. Main targets and compounds related to lipid and atherosclerosis. (A) PPI network of targets related to lipid and atherosclerosis. (B) Top 30 hub targets ranked by edge in PPI network. (C) Network of lipid and atherosclerosis-related targets-related compounds. The circle represents the target, and the rhombus represents the compound. PPI, protein-protein interaction.

actin (forward: 5′-GTCAGGTCATCACTATCGGCAAT-3′, reverse: 5′-AGAGGTCTTTACGGATGTCAACGT-3′) were synthesized by Shanghai Jierui Biotechnology Co., Ltd. The cDNA, primers, and other reagents were mixed according to the kit instructions and added to an 8-tube strip. The PCR amplification was carried out using a quantitative PCR instrument (Shanghai Hongshi Medical Technology Co., Ltd., Shanghai, China), with experimental data recorded after 2 hours of amplification.

2.6 Statistical Analysis

Statistical analyses were carried out with the software of GraphPad Prism 8.0. All results are presented as mean ± SEM. Intergroup differences were evaluated using one-way ANOVA followed by Tukey's multiple comparison test. Values of $p < 0.05$ were regarded as statistically significant.

3. Results

3.1 Predicted Compounds and Mechanisms of SDFE in Treating ALI through Network Pharmacology

624 SDFE targets were obtained via SwissTargetPrediction. Additionally, 3376 ALI targets were retrieved from the GeneCards databases. As shown in Fig. 1A, 363 SDFE targets (accounting for 58.2% of all SDFE targets) were found to be ALI-related targets, and they were defined as intersection targets. GO and KEGG pathway enrichment analyses were conducted on the intersecting genes. The 20 most statistically significant GO terms are displayed in Fig. 1B; these included response to oxygen-containing compound (GO:1901700) and cellular response to oxygen-containing compound (GO:1901701). The 20 KEGG pathways with the highest enrichment significance are presented in Fig. 1C. Lipid and atherosclerosis, and chemical carcinogenesis-reactive oxygen species were involved. These results indicated a close association with oxidation and oxidative stress. In addition, as shown in Fig. 1D,

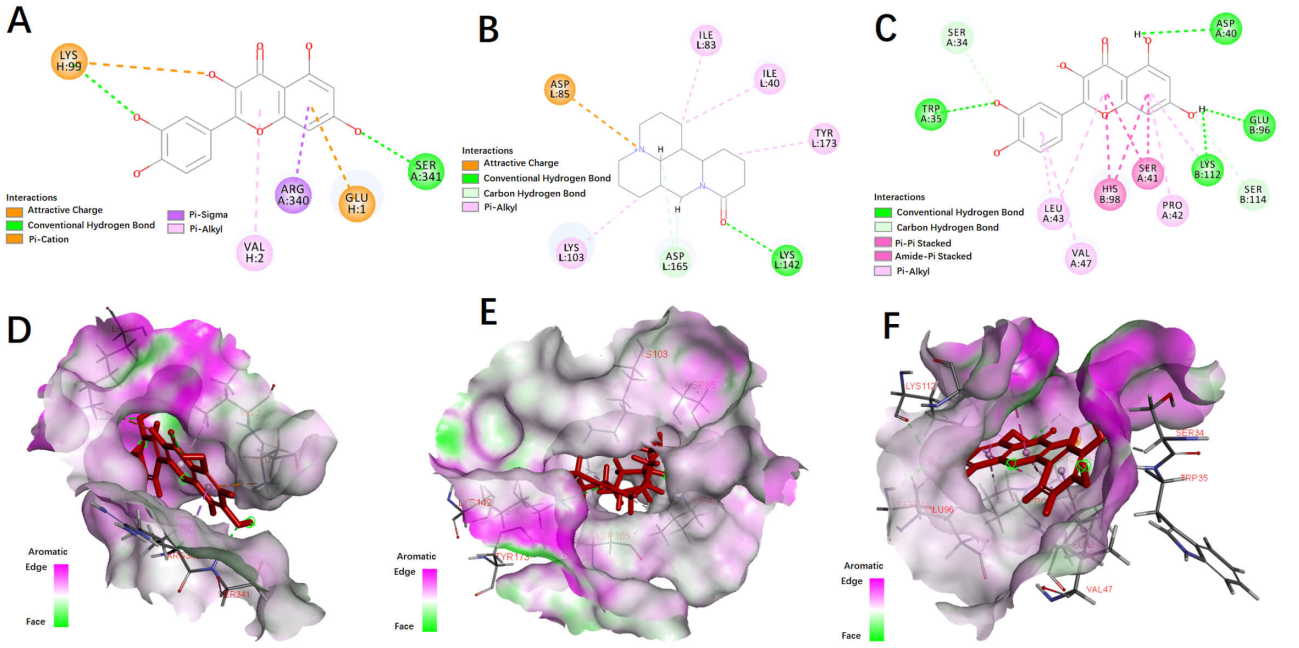

Fig. 3. Visualization of molecular docking. (A–C) 2D docking results of ICAM-1 with quercetin and matrine, and VCAM-1 with quercetin, respectively. (D–F) 3D docking results of ICAM-1 with quercetin and matrine, and VCAM-1 with quercetin, respectively. ICAM-1, intercellular adhesion molecule-1; VCAM-1, vascular cell adhesion molecule-1.

leukocyte transendothelial migration is a subpathway of lipid and atherosclerosis, its activation resulting in leukocyte adhesion and oxidative stress [20]. Thus, the pathway of lipid and atherosclerosis was selected to be investigated.

Following the identification of compounds whose targets are associated with lipid metabolism and atherosclerosis, the PPI and compound–target–pathway networks were constructed. PPI is significant for analyzing protein functions, as it reveals how proteins interact and influence each other's activities [21]. The PPI network of targets enriched in lipid and atherosclerosis was shown in Fig. 2A,B. Many targets such as AKT, PI3K, CASP3, BCL2, TNF, IKBK, MAPKs and IL1B are hub targets in the pathway of lipid and atherosclerosis, which have been studied already. Additionally, ICAM-1 (with 27 edges) and VCAM-1 (with 24 edges) are crucial for leukocyte adhesion and contribute significantly to oxidative stress. To investigate the effects of SDFE on lipid and atherosclerosis pathway, a network of KEGG pathway-target-compound was constructed using Cytoscape 3.9.0. As shown in Fig. 2C, ICAM-1 and VCAM-1 are among the top one-third targets in terms of degree values, and they have relation with main flavonoid components of SDFE, such as kaempferol and quercetin. ICAM-1 could also interact with matrine, which is one of the main alkaloid components of SDFE.

The molecular docking of proteins (ICAM-1 and VCAM-1) and their ligands (quercetin and matrine) was performed. A LibDockScore exceeding 100 suggests that the small molecule forms a stable binding with the target. The LibDockScores of quercetin and matrine with ICAM-1 are 104.215 and 101.369, respectively. The LibDockScores of quercetin with VCAM-1 are 120.185. As presented in Fig. 3A–C, multiple intermolecular interaction forces were observed between ligands and receptors. Quercetin, a flavonoid bearing several benzene rings, hydroxyl moieties, and a carbonyl group, formed stable docking complexes primarily through π–π stacking and hydrogen bonds. Fig. 3D–F demonstrate that each ligand was well enclosed in its receptor pocket constructed by π bond.

In the molecular dynamics simulations (as shown in Fig. 4), the RMSD values of the docking complexes stabilized after 10–30 ns of simulation, indicating that the protein reached a stable state upon ligand binding. The total binding free energies of the complexes ranged from –7.65 to –14.91 kcal/mol, indicating spontaneous binding between the ligands and the protein and thermodynamic stability of the complexes. These findings provide a theoretical basis at the energetic level for further investigations into the biological functions of these ligand-protein complexes.

3.2 SDFE Improves Leukocyte Adhesion and Oxidative Stress in LPS-Induced ALI Rats

3.2.1 Effects of SDFE on ALP and LDH Activities in Lung Tissue and BALF of ALI Rats

SDFE administration has been reported to mitigate both leukocyte influx and lung edema in rats with ALI or acute pneumonic injury. ALP and LDH are commonly used biomarkers for tissue damage, including acute lung injury [22]. To confirm the impact of SDFE on these biomarkers, kits were employed to measure the activities of ALP

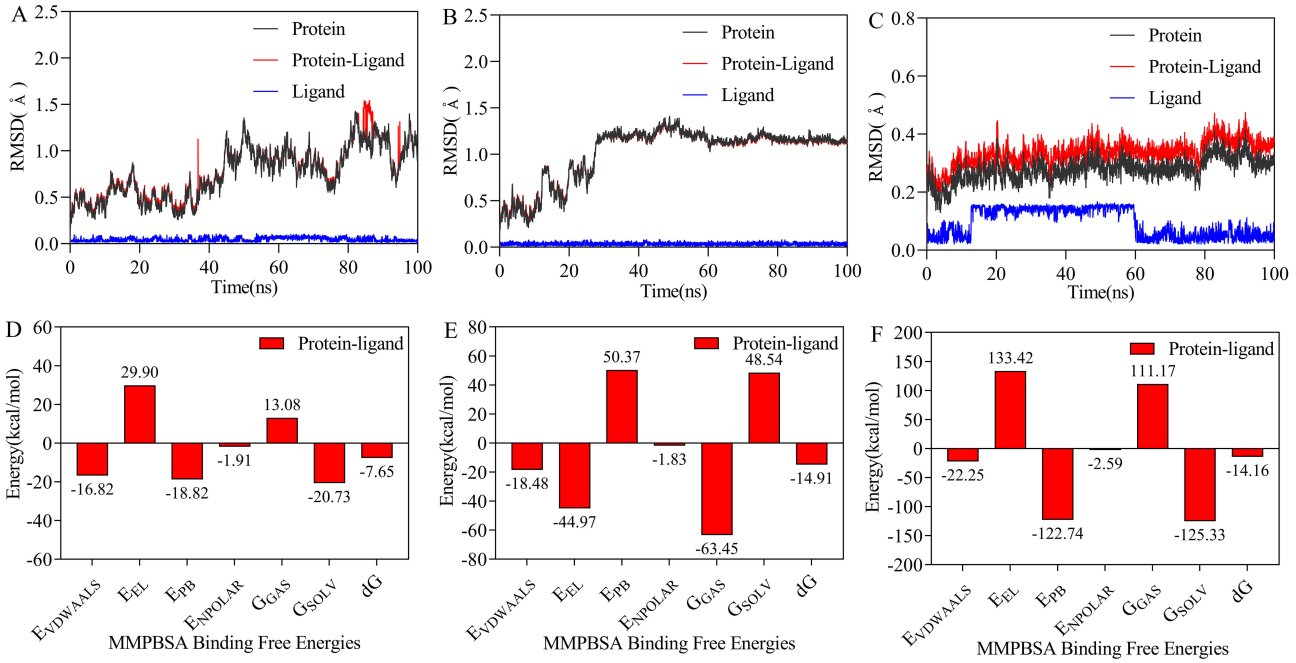

Fig. 4. Molecular dynamics simulation. (A–C) RMSD results of ICAM-1 with quercetin and matrine, and VCAM-1 with quercetin, respectively. (D–F) MMPBSA binding free energy results of ICAM-1 with quercetin and matrine, and VCAM-1 with quercetin, respectively. RMSD, root-mean-square deviation; MMPBSA, molecular mechanics poisson-boltzmann surface area.

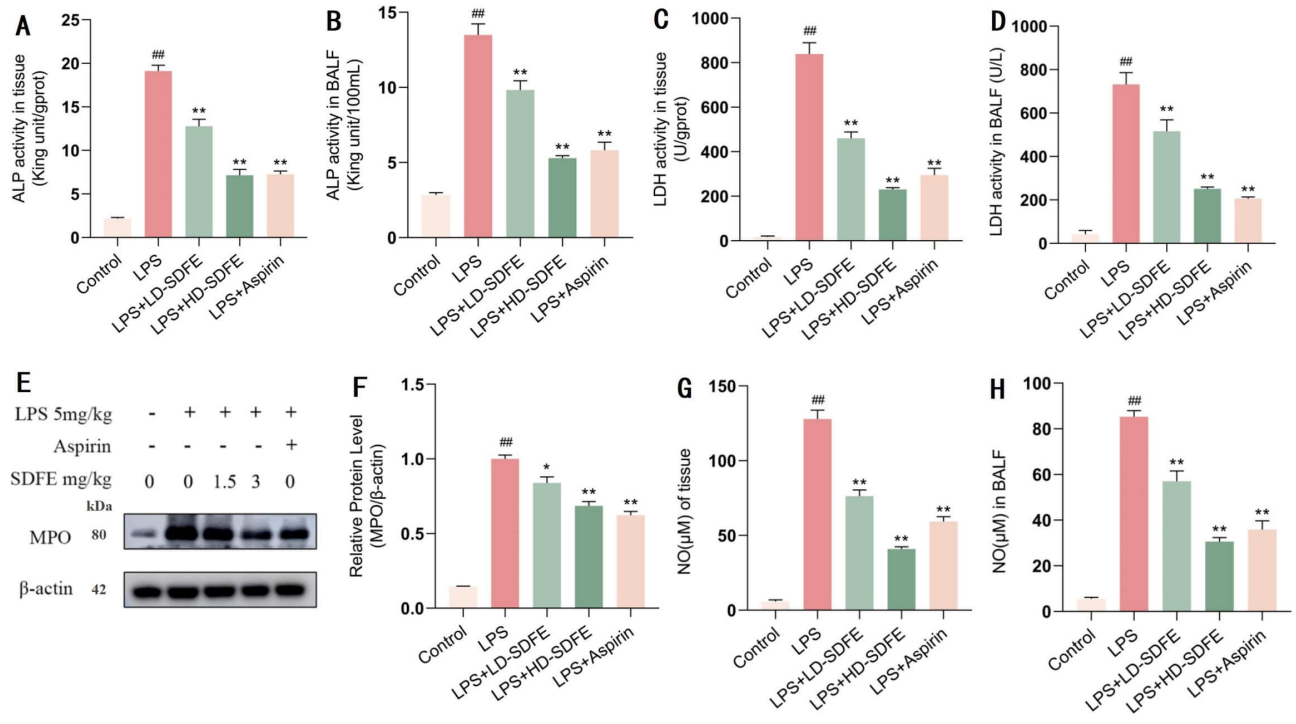

Fig. 5. Effect of SDFE on LPS- induced ALI rats. (A–D) ALP and LDH activity in rat lung tissue and BALF, respectively. Mean ± SEM, n = 6, ##$p < 0.01$ compared with the control group; **$p < 0.01$ compared with the model group. (E) Western blot of MPO protein in the rat lung. (F) Relative expression of MPO protein assayed by western blot. Mean ± SEM, n = 3. (G,H) NO level in rat lung tissue and BALF, respectively. Data are expressed as mean ± SEM (n = 6). ##$p < 0.01$ versus the control group; *$p < 0.05$ and **$p < 0.01$ versus the model group. ALP, alkaline phosphatase; LDH, lactate dehydrogenase; BALF, bronchoalveolar lavage fluid; MPO, myeloperoxidase; NO, nitric oxide.

and LDH in lung tissue and BALF from ALI rats. As shown in Fig. 5A–D, relative to the control group, the model group showed markedly elevated levels of these injury markers in both tissue specimens and BALF, confirming successful establishment of ALI. In contrast, treatment with SDFE reversed this trend, and a dose-dependent inhibition of ALP and LDH activities was observed in the SDFE-treated groups.

3.2.2 Effects of SDFE on NE, MPO, and NO Expression in Lung Tissue and BALF of ALI Rats

NE plays a crucial role in promoting cell infiltration and migration, with higher levels indicating more significant neutrophil infiltration into tissues. MPO and NO are recognized markers of oxidative stress, and their upregulation suggests the occurrence of oxidative stress, which can lead to tissue damage [23]. To further investigate the impact of SDFE on NE, MPO, and NO expression in LPS-induced ALI rats, we performed Western blot analysis to measure MPO levels in lung tissue, Griess assay to quantify NO in both lung tissue and BALF, and IHC to assess the expression of NE and MPO in lung tissue. Western blotting (Fig. 5E,F) demonstrated that LPS exposure elicited a pronounced increase in lung MPO expression compared with control animals. Conversely, SDFE treatment substantially reduced MPO abundance in a concentration-dependent fashion. In comparison with control animals, NO levels (Fig. 5G,H) were markedly elevated in the model group while SDFE treatment led to a dose-dependent reduction in NO expression. IHC results (Fig. 6A–L) demonstrated significantly higher levels of MPO and NE in model animals, which were notably reduced following SDFE treatment. These findings corroborated the western blot data regarding MPO expression.

3.3 SDFE Inhibits Leukocyte Adhesion and Oxidative Stress Activation in LPS-Induced BEAS-2B Cells

3.3.1 Effects of SDFE on ICAM-1 and VCAM-1 Expression in LPS-stimulated BEAS-2B Cells

ICAM-1 and VCAM-1 play a key role in facilitating leukocyte adhesion by binding to specific receptors on white blood cells, allowing them to traverse endothelial cells and infiltrate tissues. This process leads to the release of ROS and other oxidative stress products, which exacerbate tissue damage. To investigate the effect of SDFE on ICAM-1 and VCAM-1 expression in LPS-stimulated BEAS-2B cells, RT-qPCR was used to measure mRNA levels in the different groups. Fig. 7A,B illustrate that, relative to the control group, ICAM-1 and VCAM-1 expression were both markedly elevated in the model group. SDFE administration, however, dose-dependently attenuated the elevated levels of ICAM-1 and VCAM-1. These results indicate that SDFE inhibits the expression of ICAM-1 and VCAM-1 in LPS-stimulated BEAS-2B cells, thereby reducing leukocyte adhesion.

3.3.2 Effects of SDFE on MPO and NO Expression in LPS-stimulated BEAS-2B Cells

To investigate the effect of SDFE on MPO and NO expression in LPS-stimulated BEAS-2B cells, Western blot analysis was used to assess MPO levels, and the Griess assay was employed to measure NO content in the cell supernatants. Fig. 7C,D demonstrate that the model cohort exhibited markedly elevated levels of pro-inflammatory mediators relative to the control group. Following SDFE administration, the levels of MPO and other inflammatory mediators were dose-dependently and markedly diminished. Fig. 7E further demonstrates that LPS stimulation resulted in a significant increase in NO levels in the model group. However, SDFE treatment led to a marked reduction in NO expression, with a dose-dependent effect. The above results imply that SDFE alleviates oxidative stress levels in LPS-challenged BEAS-2B cells via inhibition of both MPO and NO expression.

4. Discussion

ALI poses significant threats to human health by impairing respiratory function and burdens society with heightened healthcare costs. SDFE can improve the ALI symptoms of leukocyte infiltration and pulmonary edema in previous investigation. In this study, SDFE exhibited a significant inhibitory effect on the tissue injury markers ALP and LDH of LPS-induced ALI rats, further indicating its therapeutic potential for ALI. ALI is closely associated with inflammation, and both inflammation and leukocyte adhesion can reciprocally activate and exacerbate each other [24,25]. Leukocyte adhesion also induces ALI via oxidative stress [26]. Network pharmacology indicated leukocyte adhesion and oxidative stress were two important signaling pathway for SDFE in the treatment of ALI. SDFE significantly suppressed NE, MPO, and NO levels in both lung tissue and BALF from LPS-induced ALI rats, and similarly reduced the mRNA expression of *ICAM-1* and *VCAM-1*, the protein expression of MPO, and the level of NO.

The transendothelial movement of leukocytes constitutes a key step during the ALI-associated inflammatory response [27,28]. This process begins when inflammatory mediators stimulate the endothelium. These activated endothelial cells express a variety of adhesion molecules, which facilitate the initial adhesion of leukocytes to the vascular endothelium [29]. Subsequently, the leukocytes migrate across the endothelial barrier into the underlying tissue, contributing to tissue inflammation and injury [30]. NE plays a critical role in leukocyte migration by degrading extracellular matrix components, thereby facilitating the movement of neutrophils through the endothelial barrier [31,32]. It has the ability to damage endothelial cells and release key adhesion molecules (such as ICAM-1 and VCAM-1) [33,34]. ICAM-1/VCAM-1 mediate the initial attachment of leukocytes to the endothelium during inflam-

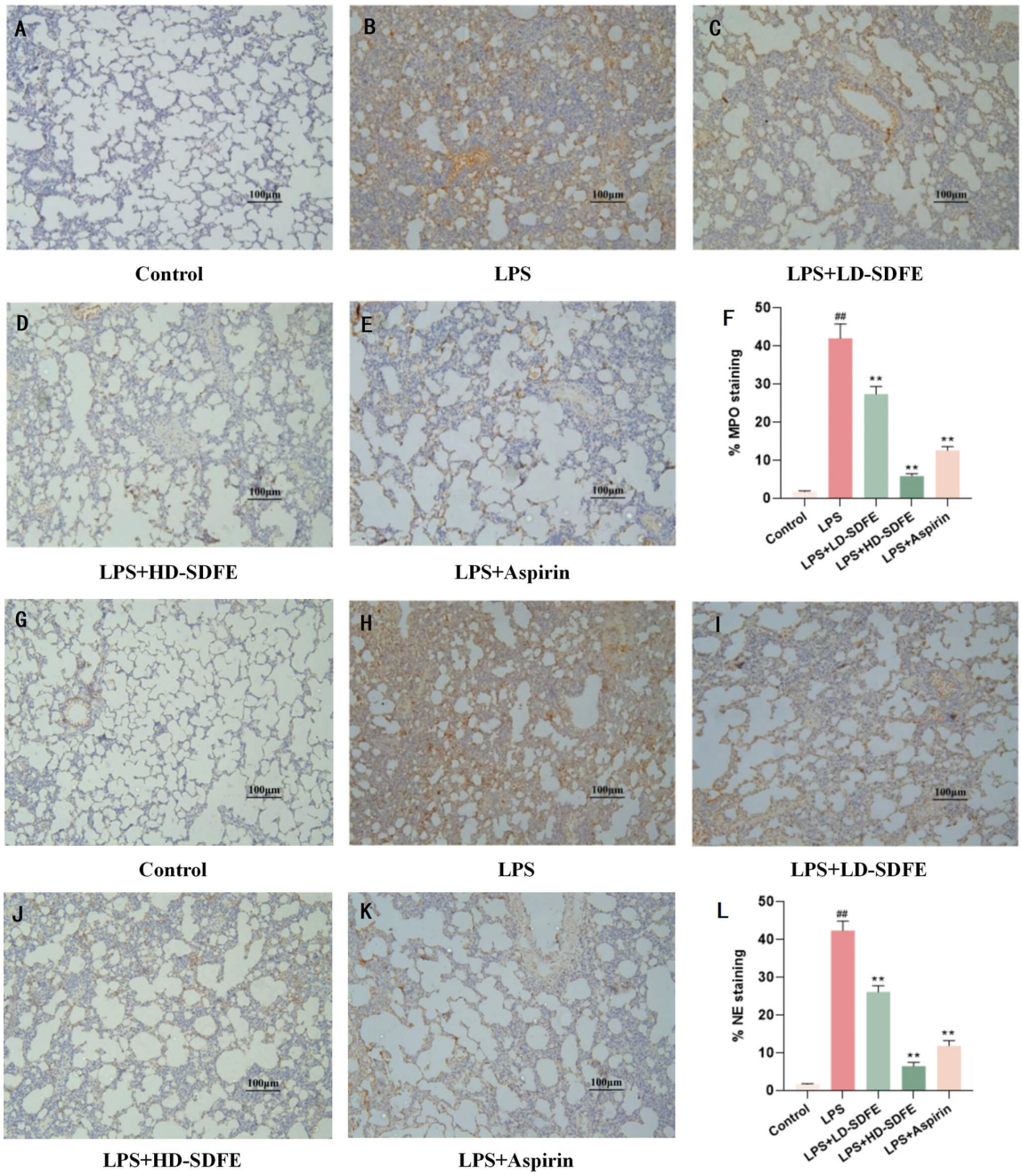

Fig. 6. IHC to detect the expression of MPO and NE in lung tissue of LPS-induced ALI rats. (A–E) IHC results of MPO of each group, respectively. (F) Relative expression of MPO in rat lung tissue. (G–K) IHC results of NE of each group, respectively. (L) Relative expression of NE in rat lung tissue. Scale bar = 100 μm. Mean ± SEM, n = 3. ##$p < 0.01$ versus the control group; **$p < 0.01$ versus the model group. IHC, immunohistochemistry; NE, neutrophil elastase.

mation [35]. The leukocytes adhesion to ICAM-1/VCAM-1 triggers the release of ROS and pro-inflammatory cytokines, further exacerbating oxidative stress and amplifying the inflammatory response [36]. This process promotes endothelial dysfunction, which exacerbates vascular permeability and worsens the development of ALI. In network pharmacology analysis, ICAM-1 and VCAM-1 are among the top one-third targets both in PPI network and lipid and atherosclerosis-related targets-related compounds network. Experiment validation indicated that SDFE could inhibit the NE expression in lung tissue and BALF of ALI rats, and down-regulate the ICAM-1/VCAM-1 expression in LPS-stimulated BEAS-2B cells.

Oxidative stress also plays a central role in the pathophysiology of ALI. ROS interact with various cellular components, leading to cellular damage and the activation of inflammatory signaling pathways [37]. The generation of ROS by activated neutrophils contributes to endothelial in-

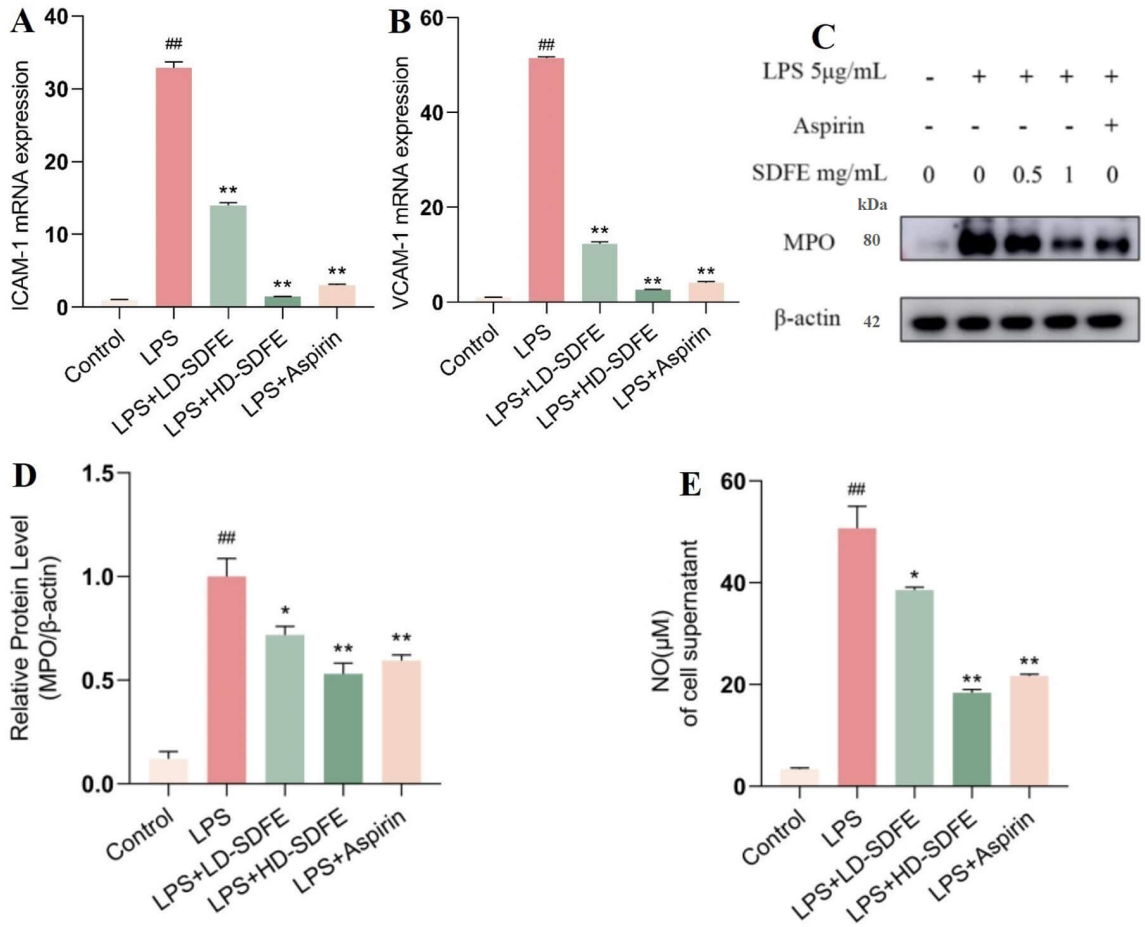

Fig. 7. Effect of SDFE on the level of ICAM-1, VCAM-1, MPO and NO in LPS-stimulated BEAS-2B Cells. (A,B) Relative mRNA expression ICAM-1 and VCAM-1, respectively. Mean ± SEM, n = 3, ##$p < 0.01$ versus the control group; **$p < 0.01$ versus the model group. (C,D) Western blot of MPO protein, and its relative expression. Mean ± SEM, n = 3. (E) NO level. Mean ± SEM, n = 6. ##$p <$ 0.01 versus the control group; *$p < 0.05$ and **$p < 0.01$ versus the model group.

jury and vascular permeability [38]. MPO is an enzyme released by neutrophils or macrophages during inflammation. MPO facilitates the production of hypochlorous acid (HOCl) using hydrogen peroxide (H_2O_2) and chloride as substrates [39]. This reaction generates highly reactive oxidants that contribute to tissue damage, endothelial dysfunction, and the recruitment of additional leukocytes to the site of injury [40]. NO is a crucial regulator of endothelial function. Some ALI-related studies have shown that under oxidative stress conditions, the activity of inducible nitric oxide synthase (iNOS) may increase, leading to the production of a large amount of NO [41]. NO interacts with ROS to form peroxynitrite, a highly reactive molecule that further damages endothelial cells and contributes ALI [42,43]. Through GO and KEGG enrichment analysis, it was found that oxidative stress was widely involved in ALI-treatment of SDFE. Experiment validation indicated that SDFE could inhibit the MPO and NO expression in lung tissue and BALF of ALI rats, and down-regulate the MPO and NO expression in LPS-stimulated BEAS-2B cells.

In this study, network pharmacology played an important role in predicting the main pathways, targets and compounds of SDFE. It provided the hypothesis that SDFE could treat ALI through the inhibition of leukocyte adhesion and oxidative stress. It is worth noting that leukocyte adhesion and oxidative stress are included in the pathway of leukocyte transendothelial migration, a subpathway of lipid and atherosclerosis. Leukocyte transendothelial migration should be paid more attention than lipid and atherosclerosis. ICAM-1/VCAM-1 were two important targets through PPI analysis and network analysis of lipid and atherosclerosis-related targets-related compounds. However, ICAM-1/VCAM-1 are not ranked among the top 3 targets. On one hand, the top 3 targets are AKT, PI3K and CASP3, which have been investigated before. On the other hand, ICAM-1/VCAM-1 are more related to leukocyte transendothelial migration. As a limitation, the binding interactions between compounds and their respective targets have only been computationally modeled through molecular docking simulations. The absence of experimen-

tal validation, such as surface plasmon resonance (SPR) or other biochemical binding assays, undermines the robustness of these predicted interactions. Future studies should aim to bridge this gap by incorporating rigorous experimental approaches.

5. Limitations

The present study provides preliminary evidence that SDFE exerts protective effects against LPS-induced ALI, potentially through inhibiting leukocyte adhesion and oxidative stress. Nevertheless, several limitations should be acknowledged. First, whether SDFE confers similar protection in ALI induced by other etiologies or in other inflammatory conditions remains to be determined. Second, the potential pharmacological activities of other parts of *Sophora davidii* (Franch.) require systematic investigation. Third, the current findings are primarily based on phenotypic observations and marker detection; causal validation via genetic intervention approaches is lacking, and the upstream signaling mechanisms by which SDFE regulates adhesion molecules and oxidative stress have not been fully elucidated. Further studies incorporating multi-omics analyses and loss-/gain-of-function experiments are warranted to identify the precise molecular targets and regulatory networks of SDFE.

6. Conclusion

In summary, this study integrates network pharmacology prediction, molecular docking simulation, and both *in vivo* and *in vitro* experimental validation to elucidate the therapeutic mechanism of SDFE in ALI. The findings demonstrate that SDFE effectively ameliorates LPS-induced ALI by targeting a dual pathogenic mechanism: the inhibition of leukocyte adhesion, as evidenced by the downregulation of NE, ICAM-1, and VCAM-1, and the suppression of oxidative stress, reflected by the reduction of MPO and NO levels. By experimentally confirming the key pathways and targets identified through computational analysis, this work not only provides a scientific basis for the traditional use of *Sophora davidii* in respiratory ailments but also highlights the value of combining network pharmacology and molecular docking simulation with empirical research in drug discovery. These results position SDFE as a promising multi-target therapeutic candidate for ALI, warranting further investigation into its clinical potential and upstream regulatory mechanisms.

Availability of Data and Materials

The essential data are documented within the article, while additional data supporting the study's conclusions are accessible from the corresponding author upon reasonable request.

Author Contributions

The project was conceptualized by LL. Experimental procedures were carried out by CL, PC, XW, DL, and BY, who also contributed to the manuscript's writing. CL was responsible for drafting the initial manuscript. LL provided manuscript revisions. LL served as corresponding authors. The final manuscript was reviewed and confirmed by all authors. Each author took part in the work sufficiently and agreed to be accountable for all aspects of the work.

Ethics Approval and Consent to Participate

All animal procedures were performed in accordance with the European Directive 2010/63/EU on the protection of animals used for scientific purposes, and were approved by the Animal Ethics Committee of Gannan Medical University (Approval No.2022048). The study was carried out in accordance with the ARRIVE guidelines. Throughout the experiments, all animals received humane care, and every procedure was carried out under the oversight of this committee.

Acknowledgment

Not applicable.

Funding

This work was supported by the Jiangxi Provincial Department of Education Science and Technology Research Project (GJJ2501316).

Conflict of Interest

The authors declare no conflict of interest.

Supplementary Material

Supplementary material associated with this article can be found, in the online version, at https://doi.org/10.31083/IJP48608.

References

[1] Long ME, Mallampalli RK, Horowitz JC. Pathogenesis of pneumonia and acute lung injury. Clinical Science (London, England: 1979). 2022; 136: 747–769. https://doi.org/10.1042/CS20210879.

[2] Butt Y, Kurdowska A, Allen TC. Acute Lung Injury: A Clinical and Molecular Review. Archives of Pathology & Laboratory Medicine. 2016; 140: 345–350. https://doi.org/10.5858/arpa.2015-0519-RA.

[3] Khemani RG, Smith L, Lopez-Fernandez YM, Kwok J, Morzov R, Klein MJ, et al. Paediatric acute respiratory distress syndrome incidence and epidemiology (PARDIE): an international, observational study. The Lancet. Respiratory Medicine. 2019; 7: 115–128. https://doi.org/10.1016/S2213-2600(18)30344-8.

[4] Janz DR, Ware LB. Biomarkers of ALI/ARDS: pathogenesis, discovery, and relevance to clinical trials. Seminars in Respiratory and Critical Care Medicine. 2013; 34: 537–548. https://doi.org/10.1055/s-0033-1351124.

[5] Lasky LA. Lectin cell adhesion molecules (LEC-CAMs): a new family of cell adhesion proteins involved with inflammation.

Journal of Cellular Biochemistry. 1991; 45: 139–146. https://doi.org/10.1002/jcb.240450204.
[6] El Alam S, Pena E, Aguilera D, Siques P, Brito J. Inflammation in Pulmonary Hypertension and Edema Induced by Hypobaric Hypoxia Exposure. International Journal of Molecular Sciences. 2022; 23: 12656. https://doi.org/10.3390/ijms232012656.
[7] Yusuf-Makagiansar H, Anderson ME, Yakovleva TV, Murray JS, Siahaan TJ. Inhibition of LFA-1/ICAM-1 and VLA-4/VCAM-1 as a therapeutic approach to inflammation and autoimmune diseases. Medicinal Research Reviews. 2002; 22: 146–167. https://doi.org/10.1002/med.10001.
[8] Liu Y, Li H, Ouyang Y, Zhang Y, Pan P. Exploration of the role of oxidative stress-related genes in LPS-induced acute lung injury via bioinformatics and experimental studies. Scientific Reports. 2023; 13: 21804. https://doi.org/10.1038/s41598-023-49165-3.
[9] Zhou J, Peng Z, Wang J. Trelagliptin Alleviates Lipopolysaccharide (LPS)-Induced Inflammation and Oxidative Stress in Acute Lung Injury Mice. Inflammation. 2021; 44: 1507–1517. https://doi.org/10.1007/s10753-021-01435-w.
[10] Fu C, Dai X, Yang Y, Lin M, Cai Y, Cai S. Dexmedetomidine attenuates lipopolysaccharide-induced acute lung injury by inhibiting oxidative stress, mitochondrial dysfunction and apoptosis in rats. Molecular Medicine Reports. 2017; 15: 131–138. https://doi.org/10.3892/mmr.2016.6012.
[11] Imai Y, Kuba K, Neely GG, Yaghubian-Malhami R, Perkmann T, van Loo G, et al. Identification of oxidative stress and Toll-like receptor 4 signaling as a key pathway of acute lung injury. Cell. 2008; 133: 235–249. https://doi.org/10.1016/j.cell.2008.02.043.
[12] Wang Q, Yan SF, Hao Y, Jin SW. Specialized Pro-resolving Mediators Regulate Alveolar Fluid Clearance during Acute Respiratory Distress Syndrome. Chinese Medical Journal. 2018; 131: 982–989. https://doi.org/10.4103/0366-6999.229890.
[13] Mokra D, Mikolka P, Kosutova P, Mokry J. Corticosteroids in Acute Lung Injury: The Dilemma Continues. International Journal of Molecular Sciences. 2019; 20: 4765. https://doi.org/10.3390/ijms20194765.
[14] Yeh CH, Yang JJ, Yang ML, Li YC, Kuan YH. Rutin decreases lipopolysaccharide-induced acute lung injury via inhibition of oxidative stress and the MAPK-NF-κB pathway. Free Radical Biology & Medicine. 2014; 69: 249–257. https://doi.org/10.1016/j.freeradbiomed.2014.01.028.
[15] Huang YC, Horng CT, Chen ST, Lee SS, Yang ML, Lee CY, et al. Rutin improves endotoxin-induced acute lung injury via inhibition of iNOS and VCAM-1 expression. Environmental Toxicology. 2016; 31: 185–191. https://doi.org/10.1002/tox.22033.
[16] Li K, Ma Y, Zhou T, Yang X, Choi HY. Chemical Constituents from Roots of *Sophora davidii* (Franch.) Skeels and Their Glucose Transporter 4 Translocation Activities. Molecules (Basel, Switzerland). 2021; 26: 756. https://doi.org/10.3390/molecules26030756.
[17] Tai Z, Cai L, Dai L, Dong L, Wang M, Yang Y, et al. Antioxidant activity and chemical constituents of edible flower of Sophora viciifolia. Food Chemistry. 2011; 126: 1648–1654. https://doi.org/10.1016/j.foodchem.2010.12.048.
[18] Chen P, Lin C, Jin Q, Ye B, Liu X, Wang K, et al. Investigating mechanisms of Sophora davidii (Franch.) skeels flower extract in treating LPS-induced acute pneumonia based on network pharmacology. Journal of Ethnopharmacology. 2025; 337: 118914. https://doi.org/10.1016/j.jep.2024.118914.
[19] Ye B, Chen P, Lin C, Zhang C, Li L. Study on the material basis and action mechanisms of sophora davidii (Franch.) skeels flower extract in the treatment of non-small cell lung cancer. Journal of Ethnopharmacology. 2023; 317: 116815. https://doi.org/10.1016/j.jep.2023.116815.
[20] Pickett JR, Wu Y, Zacchi LF, Ta HT. Targeting endothelial vascular cell adhesion molecule-1 in atherosclerosis: drug discovery and development of vascular cell adhesion molecule-1-directed novel therapeutics. Cardiovascular Research. 2023; 119: 2278–2293. https://doi.org/10.1093/cvr/cvad130.
[21] Marchand A, Van Hall-Beauvais AK, Correia BE. Computational design of novel protein-protein interactions - An overview on methodological approaches and applications. Current Opinion in Structural Biology. 2022; 74: 102370. https://doi.org/10.1016/j.sbi.2022.102370.
[22] Bruinsma BG, Wu W, Ozer S, Farmer A, Markmann JF, Yeh H, et al. Warm ischemic injury is reflected in the release of injury markers during cold preservation of the human liver. PloS One. 2015; 10: e0123421. https://doi.org/10.1371/journal.pone.0123421.
[23] Okamoto M, Mizuno R, Kawada K, Itatani Y, Kiyasu Y, Hanada K, et al. Neutrophil Extracellular Traps Promote Metastases of Colorectal Cancers through Activation of ERK Signaling by Releasing Neutrophil Elastase. International Journal of Molecular Sciences. 2023; 24: 1118. https://doi.org/10.3390/ijms24021118.
[24] McVey MJ, Steinberg BE, Goldenberg NM. Inflammasome activation in acute lung injury. American Journal of Physiology. Lung Cellular and Molecular Physiology. 2021; 320: L165–L178. https://doi.org/10.1152/ajplung.00303.2020.
[25] Peng F, Yin H, Du B, Niu K, Yang Y, Wang S. Anti-inflammatory effect of flavonoids from chestnut flowers in lipopolysaccharide-stimulated RAW 264.7 macrophages and acute lung injury in mice. Journal of Ethnopharmacology. 2022; 290: 115086. https://doi.org/10.1016/j.jep.2022.115086.
[26] Kar S, Kavdia M. Computational model for oxidative and nitrosative stress for endothelial dysfunction related leukocyte adhesion and transmigration. The FASEB Journal. 2011; 25: 63813. https://doi.org/10.1096/fasebj.25.1_supplement.638.13.
[27] Schimmel L, Heemskerk N, van Buul JD. Leukocyte transendothelial migration: A local affair. Small GTPases. 2017; 8: 1–15. https://doi.org/10.1080/21541248.2016.1197872.
[28] Nourshargh S, Hordijk PL, Sixt M. Breaching multiple barriers: leukocyte motility through venular walls and the interstitium. Nature Reviews. Molecular Cell Biology. 2010; 11: 366–378. https://doi.org/10.1038/nrm2889.
[29] Grönloh MLB, Arts JJG, van Buul JD. Neutrophil transendothelial migration hotspots - mechanisms and implications. Journal of Cell Science. 2021; 134: jcs255653. https://doi.org/10.1242/jcs.255653.
[30] Lyck R, Enzmann G. The physiological roles of ICAM-1 and ICAM-2 in neutrophil migration into tissues. Current Opinion in Hematology. 2015; 22: 53–59. https://doi.org/10.1097/MOH.0000000000000103.
[31] Smedly LA, Tonnesen MG, Sandhaus RA, Haslett C, Guthrie LA, Johnston RB, Jr, et al. Neutrophil-mediated injury to endothelial cells. Enhancement by endotoxin and essential role of neutrophil elastase. The Journal of Clinical Investigation. 1986; 77: 1233–1243. https://doi.org/10.1172/JCI112426.
[32] Raevens S, Van Campenhout S, Debacker PJ, Lefere S, Verhelst X, Geerts A, et al. Combination of sivelestat and N-acetylcysteine alleviates the inflammatory response and exceeds standard treatment for acetaminophen-induced liver injury. Journal of Leukocyte Biology. 2020; 107: 341–355. https://doi.org/10.1002/JLB.5A1119-279R.
[33] Champagne B, Tremblay P, Cantin A, St Pierre Y. Proteolytic cleavage of ICAM-1 by human neutrophil elastase. Journal of Immunology (Baltimore, Md.: 1950). 1998; 161: 6398–6405.
[34] Lévesque JP, Takamatsu Y, Nilsson SK, Haylock DN, Simmons PJ. Vascular cell adhesion molecule-1 (CD106) is cleaved by neutrophil proteases in the bone marrow following hematopoietic progenitor cell mobilization by granulocyte colony-stimulating factor. Blood. 2001; 98: 1289–1297. https:

//doi.org/10.1182/blood.v98.5.1289.
[35] Staunton DE, Dustin ML, Erickson HP, Springer TA. The arrangement of the immunoglobulin-like domains of ICAM-1 and the binding sites for LFA-1 and rhinovirus. Cell. 1990; 61: 243–254. https://doi.org/10.1016/0092-8674(90)90805-o.
[36] Cook-Mills JM. VCAM-1 signals during lymphocyte migration: role of reactive oxygen species. Molecular Immunology. 2002; 39: 499–508. https://doi.org/10.1016/s0161-5890(02)00206-7.
[37] Lum H, Roebuck KA. Oxidant stress and endothelial cell dysfunction. American Journal of Physiology. Cell Physiology. 2001; 280: C719–C741. https://doi.org/10.1152/ajpcell.2001.280.4.C719.
[38] Fortuño A, San José G, Moreno MU, Díez J, Zalba G. Oxidative stress and vascular remodelling. Experimental Physiology. 2005; 90: 457–462. https://doi.org/10.1113/expphysiol.2005.030098.
[39] Lin W, Chen H, Chen X, Guo C. The Roles of Neutrophil-Derived Myeloperoxidase (MPO) in Diseases: The New Progress. Antioxidants (Basel, Switzerland). 2024; 13: 132. https://doi.org/10.3390/antiox13010132.
[40] Zhan Z, Lei Q, Dai Y, Wang D, Yu Q, Lv Y, et al. Simultaneous Monitoring of HOCl and Viscosity with Drug-Induced Pyroptosis in Live Cells and Acute Lung Injury. Analytical Chemistry. 2022; 94: 12144–12151. https://doi.org/10.1021/acs.analchem.2c02235.
[41] El-Awady MS, Said E, Baraka HN. Acylated catalpol diglycoside ameliorates lipopolysaccharides-induced acute lung injury through inhibition of iNOS and TNF-α expression. Journal of Biochemical and Molecular Toxicology. 2018; 32: e22214. https://doi.org/10.1002/jbt.22214.
[42] Zhou X, Ding X, Shen J, Yang D, Hudson LG, Liu KJ. Peroxynitrite contributes to arsenic-induced PARP-1 inhibition through ROS/RNS generation. Toxicology and Applied Pharmacology. 2019; 378: 114602. https://doi.org/10.1016/j.taap.2019.114602.
[43] Li C, Gui P, He X, Yang H. Actions of NO and INOS on endotoxin induced rat acute lung injury and effect of rhubarb on them. Journal of Traditional Chinese Medicine = Chung i Tsa Chih Ying Wen Pan. 2000; 20: 216–222.